Gauss's Law Test of Gravity at Short Range

M. V. Moody and H. J. Paik

Department of Physics and Center for Superconductivity Research, University of Maryland, College Park, Maryland 20742

(Received 2 October 1992)

A null test of the gravitational inverse-square law can be performed by testing Gauss's law for the field. We have constructed a three-axis superconducting gravity gradiometer and carried out such a test. A lead pendulum weighing 1500 kg was used to produce a time-varying field. This experiment places a new (2σ) limit of $\alpha=(0.9\pm4.6)\times10^{-4}$ at $\lambda=1.5$ m, where α and λ are parameters for the generalized potential $\phi=-(GM/r)(1+\alpha e^{-r/\lambda})$.

PACS numbers: 04.90.+e, 04.80.+z

Various types of light-mass bosons have been suggested to answer open questions in particle physics and gravity. The presence of these bosons would give rise to a Yukawa-type potential and thus appear as a violation of the gravitational inverse-square law. Numerous experiments have been performed to search for a composition-dependent as well as a composition-independent violation of the inverse-square law [1]. The experiment reported here is unique in that it employs a new instrument, a superconducting gravity gradiometer (SGG), and is based on a new approach, a test of Gauss's law for gravity. The result is $\alpha=(0.9\pm4.6)\times10^{-4}$ at $\lambda=1.5$ m, where $\phi=-(GM/r)(1+\alpha e^{-r/\lambda})$ and the error corresponds to a 2σ level. This represents an improvement of 2 orders of magnitude over our previous result [2] and more than an order of magnitude over the best existing limit [3].

A differential equivalent of the inverse-square force law is Gauss's law for the field, $\nabla\cdot\mathbf{g}=-4\pi G\rho$, where $\mathbf{g}=-\nabla\phi$. By summing the outputs of an in-line gravity gradiometer rotated into three orthogonal directions, one can perform a near null test of the inverse-square law. The advantage of this type of experiment is its reduced sensitivity to the source density and metrology errors [4]. The residual sensitivity to the source errors results from higher moments of the gradiometer which couple to higher-order field gradients.

Each axis of the SGG consists of two spring-mass accelerometers in which the proof masses are confined to motion in a single degree of freedom along a common axis, and are coupled together by superconducting circuits. Platform motions that are common to both accelerometers are canceled by adjusting the ratio of two persistent currents in the sensing circuit. The sensing circuit is connected to a commercial SQUID amplifier to sense changes in the persistent currents generated by differential accelerations, i.e., gravity gradients. A second sensing circuit is used to sense common accelerations. The design and analysis of this gradiometer have been previously published [5].

A three-axis gravity gradiometer is formed by mounting six accelerometers on the faces of a precision cube. The accelerometers on two opposite faces of the cube form one of three in-line gradiometers. Aligning the diagonal of the cube with the vertical equally biases the three gradiometer axes with respect to the Earth's gravitational acceleration (see Fig. 1). This orientation also permits the cyclic interchange of the gradiometer axes by a 120° rotation about the vertical.

In a perfect gradiometer the platform accelerations could be canceled to the degree to which the persistent currents could be adjusted. In actuality, the sensitive axes of the component accelerometers are not perfectly aligned. This misalignment results in a residual coupling to platform motion. The gradiometer alignment errors can be described in terms of a misalignment between the directions of the sensitive axes, $\delta\hat{\mathbf{n}}=\hat{\mathbf{n}}_2-\hat{\mathbf{n}}_1$, and a misalignment between the average direction of the sensitive axes and the baseline vector, $\delta\hat{\boldsymbol{l}}=(\hat{\mathbf{n}}_1+\hat{\mathbf{n}}_2)/2-\hat{\boldsymbol{l}}$. The gradiometer couples to translational accelerations and tilt through $\delta\hat{\mathbf{n}}$, whereas $\delta\hat{\boldsymbol{l}}$ results in coupling to angular acceleration [6]. The errors in sensitive axes alignment will also result in a misorientation of the gradiome-

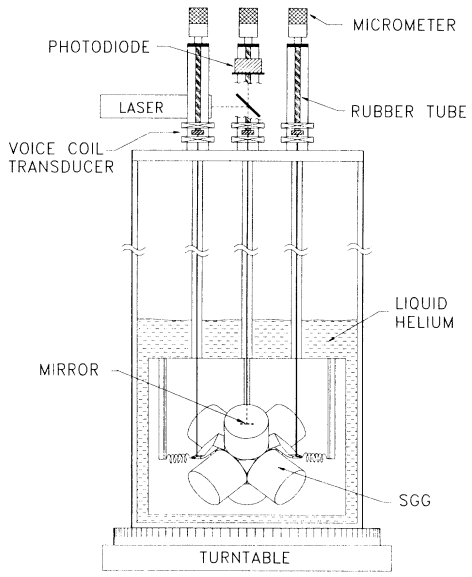

FIG. 1. Schematic side view of the SGG and supporting hardware. The laser beam passes down a center tube (not shown) in the cryostat. The three vertical supports are symmetric relative to the center tube.

ter axes, $\delta\hat{\mathbf{x}}$. This error will result in an error in the orthogonality among the three in-line gradiometers and among the cyclic orientations for an individual gradiometer axis.

Even in a perfectly aligned gradiometer, angular motion about an axis other than its own sensitive axis produces centrifugal acceleration errors. If the gradiometer platform is stationary in the Earth's reference frame, the centrifugal acceleration error is given by $2[(\hat{\mathbf{n}}\cdot\boldsymbol{\Omega}_E)\times(\hat{\mathbf{n}}\cdot\delta\boldsymbol{\Omega}_p)+\boldsymbol{\Omega}_E\cdot\delta\boldsymbol{\Omega}_p]$, where $\boldsymbol{\Omega}_E$ is the angular velocity of the Earth and $\delta\boldsymbol{\Omega}_p$ is the angular jitter of the platform [6].

To perform the experiment, the gradiometer is rotated twice by 120° about the vertical to obtain a measurement of $\nabla\cdot\mathbf{g}$ with each gradiometer axis. The sum of the three cyclic orientations j of gradiometer axis i is given [7] by

$$\sum_j \Gamma_i^{(j)} = (1+\epsilon_i)\left\{3\sqrt{3}(\hat{\mathbf{z}}\cdot\boldsymbol{\Gamma}\cdot\hat{\mathbf{z}})(\delta\hat{\mathbf{x}}_i\cdot\hat{\mathbf{z}})+2\boldsymbol{\Omega}^2-\frac{\sqrt{3}}{2}[3(\boldsymbol{\Omega}\cdot\hat{\mathbf{z}})^2-\boldsymbol{\Omega}^2](2\delta\hat{\mathbf{x}}_i\cdot\hat{\mathbf{z}}+\delta\hat{\boldsymbol{l}}_i\cdot\hat{\mathbf{z}})-3(\dot{\boldsymbol{\Omega}}\cdot\hat{\mathbf{z}})[(\delta\hat{\boldsymbol{l}}_i\times\hat{\mathbf{n}}_i)\cdot\hat{\mathbf{z}}]\right.$$
$$\left.-\frac{3}{l}(\ddot{\mathbf{r}}+\mathbf{g})\cdot\hat{\mathbf{z}}(\delta\hat{\mathbf{n}}_i\cdot\hat{\mathbf{z}}+\delta h_i/\sqrt{3})\right\}. \quad (1)$$

Here, ϵ is the error in the gradiometer scale factor, $\boldsymbol{\Gamma}$ is the gravity gradient tensor, $\boldsymbol{\Omega}=\boldsymbol{\Omega}_E+\delta\boldsymbol{\Omega}_p$, $\ddot{\mathbf{r}}$ represents the acceleration of the platform, $\mathbf{g}$ represents the gravitational acceleration, l is the gradiometer baseline, and δh is the persistent current misbalance. This result indicates that, after summing over the three orthogonal orientations, only the vertical components of the error terms are significant.

Figure 1 shows a schematic of the apparatus. The SGG is composed of six cylindrical accelerometers, 10.2 cm in diameter and 8.9 cm long, mounted on a cube, 10.2 cm on a side. It is cooled inside an Al vacuum can with liquid helium contained in a vapor-cooled cryostat. Magnetic isolation consists of the SGG niobium (Nb) accelerometer housings, two layers of superconducting Pb shield, and a double wall Mumetal shield at room temperature. The vibration isolation of the SGG is passive and consists of three vertical suspension legs, and three springs located in the horizontal plane passing through the SGG center of mass. These springs increase the horizontal and torsional resonance frequencies of the SGG isolation to well above the signal frequency. The primary purpose of the vibration isolation is to reduce SGG platform motions at frequencies where the seismic noise can cause overloading of the SQUID amplifiers. Voice-coil type transducers are incorporated into each leg of the suspension. By varying the magnitude and phase of the currents through the coils, vertical motion or tilt (in any direction) may be applied to the SGG. The tilt motion is sensed with a two-dimensional optical lever consisting of a laser, a beam splitter, an x-y photodiode at room temperature, and a flat mirror mounted on the SGG cube (perpendicular to the diagonal). The cryostat and Mumetal shields rest upon a turntable driven by a stepper motor. The rotational accuracy of the turntable was determined to be better than 10^{-4} rad.

Since we are approximating the gradient by subtracting acceleration over a finite (nonzero) baseline l, 0.1905 $\pm$0.0003 m, there is a residual Newtonian term that must be removed to obtain $\nabla\cdot\mathbf{g}$. Errors in the source metrology limit the accuracy to which this term can be removed. The source used in this experiment is a 1498 $\pm$ 3 kg pendulum confined to a single plane of motion by an Al tube and bearings at the pivot. The pendulum mass is a 0.324 m diam, 0.0064 m thick spherical Al shell with a Pb core. The eccentricity of this mass is less than 0.01. The distance between the pendulum pivot and the center of the sphere is 3.300 $\pm$ 0.005 m. The position of the pendulum is obtained using a 13 bit optical shaft encoder attached to one end of the pivot shaft. The amplitude of the pendulum is maintained to within $\pm$0.0004 rad ($\pm$0.5 bit) per cycle by a pneumatic drive attached to the other end of the pivot shaft. The vertical and horizontal positions of the pendulum pivot relative to the SGG center were 4.583 $\pm$ 0.003 and 4.235 $\pm$ 0.003 m, respectively. The turntable, SGG mirror, and pendulum pivot were leveled to better than 0.0002 rad. The pendulum's plane of motion was aligned with the center of the turntable to better than 0.0002 rad. A numerical model of the experiment, in which the SGG accelerometers were modeled as point masses confined to a single degree of freedom, and the source was modeled as a simple pendulum, gives $(-4.04\pm0.11)\times10^{-3}$ E (1 E$\equiv10^{-9}$ s^{-2}) for the residual term due to the finite baseline.

When the gradiometer axes are permuted by rotating the turntable, a displacement of the center of mass of the SGG, δr, leads to an error in the measurement of $\nabla\cdot\mathbf{g}$. The SGG was centered on the turntable rotation axis by observing the SGG mirror with a transit as the turntable was rotated through 360°. The resolution of this measurement, $\pm$0.0004 m, places an upper bound on δr. The numerical model indicates the error due to δr is minimized when the initial turntable orientation ϕ_I is such that the sensitive axis of one gradiometer is in the pendulum's plane of motion pointing away from the pendulum. This orientation (denoted as 0°) was chosen for the experiment resulting in an upper bound of 1.34×10^{-4} E for this displacement induced error.

The model was also used to investigate and minimize the SGG nonorthogonality error. Equation (1) indicates that this is accomplished by minimizing Γ_{ZZ}. If, as in the present experiment, the analysis is limited to measurements at the pendulum frequency f_p of 0.2681 $\pm$ 0.0001 Hz, then only the fundamental component of Γ_{ZZ} contributes to the error. The vertical gradient, Γ_{ZZ}, of the

source as a function of SGG polar angle has a zero at 54.74°. By positioning the pendulum so that at its maximum amplitude of 34.06° the mass is at a polar angle of 54.23°, we were able to reduce the fundamental component of Γ_{ZZ} to 0.009 E.

Equation (1) shows that the torsional acceleration of the platform, $\dot{\boldsymbol{\Omega}}\cdot\hat{\mathbf{z}}$, couples to the measurement of $\nabla\cdot\mathbf{g}$ through the z component of $\delta\hat{\boldsymbol{l}}\times\hat{\mathbf{n}}$. To make an accurate determination of this component, the torsional mode of the SGG platform was excited using the turntable. This motion results in a peak in the power spectrum at the torsional frequency, f_t, due to $(\delta\hat{\boldsymbol{l}}\times\hat{\mathbf{n}})_z$, and a second peak at $2f_t$ due to centrifugal acceleration. The magnitude of the $2f_t$ peak gives a measure of the torsional motion amplitude. Combining this with the magnitude of the f_t peak, we obtain $(\delta\hat{\boldsymbol{l}}\times\hat{\mathbf{n}})_z=(2.72\pm0.03)\times10^{-4}$, $(0.59\pm0.03)\times10^{-4}$, and $(-0.77\pm0.03)\times10^{-4}$ for axes 1, 2, and 3, respectively. To measure $\dot{\boldsymbol{\Omega}}\cdot\hat{\mathbf{z}}$, a ring laser gyro (RLG) was mounted to the turntable with its sensitive axis vertical. Since the SGG platform modes are much higher than the source frequency, this measurement of the torsional motion of the turntable should translate directly to the SGG platform. The RLG data were recorded and analyzed in the same manner as the SGG data discussed below. Calibration of the RLG was achieved using the Earth's rotation. A total of 130 sets of 254 records was recorded over a span of 14 days. Analysis of these data gave a torsional motion amplitude of $(3.22\pm0.09)\times10^{-9}$ rad at f_p in phase with the source. The quoted error is 2 standard deviations of the 130 sets.

In order that the gradiometer noise not be limited by seismic noise, sensitivity to acceleration must be minimized. Sensitivity to vertical acceleration is minimized by shaking the SGG vertically and adjusting the ratio of the persistent currents in the differential-mode sensing loops to null the outputs. To extend this balance to three dimensions, the SGG is tilted with amplitude θ in 2 degrees of freedom at a frequency f [$\ll(2\pi)^{-1}(g_E/l)^{1/2}\cong1$ Hz] so that the translational acceleration error ($\propto\theta g_E/l$) dominates the angular acceleration error [$\propto\theta(2\pi f)^2$]. This permits determination of the components of the $\delta\hat{\mathbf{n}}$'s. A three-dimensional balance against acceleration is then achieved by combining each gradiometer output, Γ_i', with the acceleration outputs, G_j, according to $\Gamma_i'+\sum_j s_{ij}G_j$, where the coefficients s_{ij} are determined from the $\delta\hat{\mathbf{n}}$'s. After performing this balance, the noise performance of the SGG was approximately 0.07 E Hz$^{-1/2}$ at f_p. The tilt measurements also permit absolute calibration of the accelerometer outputs.

For the experiment, the three gradient and three acceleration outputs from the SGG were recorded along with the pendulum position for 33 nights. The turntable was automatically rotated 120° twice each night. After acquisition, the data were time averaged, using the pendulum position as a reference, with a record length of six pendulum cycles. Approximately 710 records were obtained per orientation per night. The dominant analog filter was a 1.6 Hz, low pass, 8 pole butterworth. During the averaging, unlocks in the SQUID amplifiers were detected, and the record in which the unlock occurred was rejected. To minimize effects of people in the laboratory, all records with a gradient fast Fourier transform value at f_p more than 5 standard deviations from the mean were also rejected. These two rejection criteria resulted in a loss of about 0.2% of the data.

The SGG acceleration data reveal the motion of the SGG platform induced by the source. A power spectrum of these data shows that, upon summation of the three cyclic orientations, the platform acceleration is below the random noise level at the fundamental signal frequency. This result indicates that translational acceleration effects generated by the pendulum at f_p contain no significant vertical component.

Figure 2 shows that gradiometer output of axis 1 over six cycles of the pendulum for each of the three orientations and their sum. The remaining structure in the sum is primarily in the second and fourth harmonics, and is due to residual coupling to the vertical motion of the laboratory induced by the pendulum at these frequencies. The standard deviations of the three gradiometer outputs (after summing over the three cyclic orientations) for the 33 nights of data were 1.81×10^{-4}, 7.15×10^{-4}, and 1.70×10^{-4} E for axes 1, 2, and 3, respectively. For axes 1 and 3, the 33 data sets exhibited a Gaussian distribution and the standard deviations compared favorably with the short term power spectral density noise value of 0.07 E Hz$^{-1/2}$. The data from axis 2 exhibited a drift of 2.9σ over the 33 data sets. The drift for axes 1 and 3 was 1.4σ and 0.9σ, respectively. Large changes in the current balance were observed for axis 2, requiring that it be rebal-

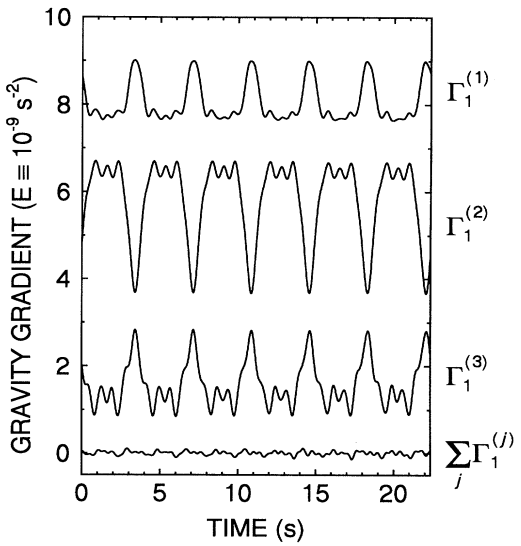

FIG. 2. The output of the differential mode sensing circuit of axis 1 for each of the three orientations and their sum. The time axis covers six cycles of the pendulum. The dc level is arbitrary.

TABLE I. Dominant errors.

Error source	2σ level (rms) (E)
Random	2.48×10^{-4}
Gradiometer rotation axis	$\leq 0.95\times10^{-4}$
Gradiometer axis nonorthogonality	$\leq 0.40\times10^{-4}$
Residual torsional acceleration	1.12×10^{-4}
Source metrology	1.08×10^{-4}
Magnetic coupling	$\leq 10^{-7}$
Total	3.1×10^{-4}

anced several times over the course of the experiment. No such problem was observed for axes 1 and 3. There is some evidence of a systematic effect arising from the large dc current induced in the loop containing the SQUID input coil, which would result from a leakage of the magnetic flux out of a sensing circuit loop. Consequently, we feel the data from this axis are substantially less reliable than that from axes 1 and 3, and our final result is given using only the two stable axes.

In addition to 33 nights of data in the 0°, 120°, and 240° orientations, 3 nights of data were recorded in the 60°, 180°, and 300° orientations. Summing the data at the 0° and 180° orientations for each axis eliminates residual coupling to horizontal and tilt motion of the floor, the dominant measurement error. Comparing the result with the value predicted by the model allows calibration of the SGG to better than 0.5%. Taking into account the torsional motion error would improve the calibration accuracy; however, the near null nature of this experiment makes further improvement unnecessary.

After time averaging the 33 data sets, the data are Fourier transformed, using a Hanning window, and separated into components in-phase (real) and out-of-phase (imaginary) with the source. These results are $(3.59-1.31i)\times10^{-3}$, $(-1.88-2.26i)\times10^{-3}$, and $(-6.22-1.18i)\times10^{-3}$ E for axes 1, 2, and 3, respectively. As previously discussed, a quadrature component will arise from centrifugal acceleration due to angular motion of the platform mixing with the Earth's rotation. Thus the out-of-phase component should agree for the different axes, and it is within 1 standard deviation for the two stable axes, 1 and 3.

After subtracting the term due to torsional motion of the floor, the sum of the gradients in the three orientations is $(-3.87\pm0.45)\times10^{-3}$ E for axis 1 and $(-4.10\pm0.37)\times10^{-3}$ E for axis 3. Thus the two axes agree. Taking a simple average of these two axes reduces the relative contribution of the $\delta\mathbf{r}$ and $\delta\hat{I}$ errors, and gives, after subtracting the finite baseline term, our final result of $(0.58\pm3.10)\times10^{-4}$ E.

The error budget for this result is given in Table I. The random noise comes from the scatter of the $\sum\Gamma_i$ data. The gradiometer rotation axis error represents an upper limit corresponding to the worst case in the direction and magnitude of $\delta\mathbf{r}$. The axis nonorthogonality error is computed from the model using the maximum error in the polar angle, 0.001 rad. The residual torsional acceleration error comes from the scatter of the RLG data. The source metrology error arises from the uncertainties in the geometric parameters that are used in the numerical model. The magnetic coupling error has been obtained by combining a null response of the gradiometer to an applied, time-varying field with the estimated residual magnetic contamination of the pendulum mass.

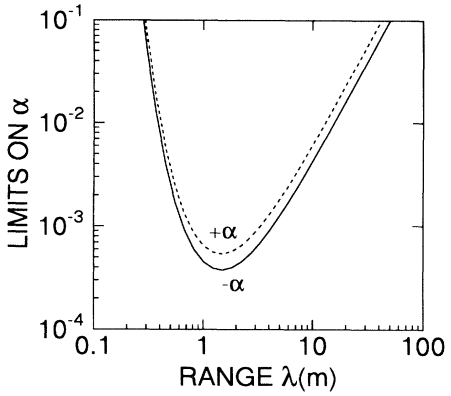

FIG. 3. 2σ limits on the Yukawa coupling constant set by this experiment.

Figure 3 shows the 2σ limits on a positive and negative α vs λ. The strictest limits are obtained at $\lambda=1.5$ m and are $\alpha=(0.9\pm4.6)\times10^{-4}$. Table I shows that the total error could be reduced by a factor of 3 by improving the random noise of the gradiometer and the gyro. A much more substantial improvement on the result can be achieved with the construction of an improved source. We are in the process of designing a near null source that does not shake the building.

This work was supported in part by the National Aeronautics and Space Administration under Contract No. NAS 8-38137, and by the U.S. Air Force under Contract No. F19628-87-K-0053. We are indebted to Lieutenant Colonel Gerry Shaw of Phillips Laboratory and Fred Nadeau of Wright Laboratories for providing the RLG and to Randell Jaffe of Rockwell International for assisting us in its operation. We gratefully acknowledge important contributions from Qin Kong, Joel Parke, Ed Canavan, Hans Haucke, and Ruozeng Liu.

[1] For a review, see E. G. Adelberger *et al.*, Annu. Rev. Nucl. Part. Sci. **41**, 269 (1991), or E. Fischbach and C. Talmadge, Nature (London) **356**, 207 (1992).
[2] H. A. Chan, M. V. Moody, and H. J. Paik, Phys. Rev. Lett. **49**, 1745 (1982).
[3] J. K. Hoskins *et al.*, Phys. Rev. D **32**, 3084 (1985).
[4] H. J. Paik, Phys. Rev. D **19**, 2320 (1979).
[5] M. V. Moody, H. A. Chan, and H. J. Paik, J. Appl. Phys. **60**, 4308 (1986).
[6] H. A. Chan and H. J. Paik, Phys. Rev. D **35**, 3551 (1987).
[7] J. W. Parke, Ph.D. thesis, University of Maryland, College Park, Maryland, 1990 (unpublished).